O-Atom Transfer to Fe_n^+ Clusters ($n = 2-10$) from O_2, N_2O and CO_2: "Microoxides of Iron"**

Oliver Gehret and Manfred P. Irion*

Abstract: We report on the gas phase reactions of small Fe_n^+ clusters ($n = 2-10$) with O_2, N_2O and CO_2 in an FT-ICR mass spectrometer. Under our experimental conditions, clusters of all sizes reacted readily with O_2 and all but the dimer reacted with N_2O. Only the smallest Fe_n^+ clusters ($n = 2-4$) appeared to activate CO_2. For all X–O molecules (X = O, N_2, CO), reaction pathways were observed that include the transfer of O atoms. In addition, the reactions with O_2 and N_2O were accompanied by the loss of one or two Fe atoms. Thermochemical considerations based upon the well-known X–O bond energies were used to calculate Fe_n–O^+ bond dissociation energies (BDEs) for sizes $n = 2-6$; these amount to roughly 550 kJ mol^{-1} and thus are considerably higher than the BDE of the Fe–O^+ ion. All oxidation reactions of the Fe_n^+ clusters ($n = 2-6$) studied in more detail were terminated by products of $Fe_xO_x^+$ stoichiometry ($x = 1-4$). These "*microoxides of iron*" are not able to activate any further X–O bonds. Secondary reactions of $Fe_xO_x^+$ clusters with C_6H_6, C_2H_4 and NH_3 were investigated for two selected sizes ($x = 2$, 3) and compared with reactions of the naked Fe_n^+ clusters.

Keywords
clusters · gas-phase chemistry · ion molecule reactions · iron complexes · mass spectrometry

Introduction

Metal clusters are characterised by a high proportion of surface atoms. Therefore, the reactivity of metal clusters towards different molecules should provide information about surfaces on a microscopic scale.

To date, numerous investigations of the gas-phase chemistry of bare transition-metal clusters have been carried out. In most cases, reactions with simple hydrocarbons have been studied, which exhibited in part C–C and C–H bond activation.[1] The observed reaction pathways often consist of several sequential steps where the addition of a hydrocarbon ligand may be accompanied by the loss of one or more H_2 molecules. An interesting aspect is the size selectivity shown by many reaction systems. One cluster size or one particular cluster ligand stoichiometry may possess properties that neighbouring sizes do not.

Compared with the reactions with hydrocarbons, there have been few efforts to study the oxidation of small metal clusters. In the case of atomic transition-metal ion chemistry, C–C and C–H bond activation by transition-metal mediated oxidation of hydrocarbons is the subject of current investigations.[2] It should be interesting to check how efficient transition-metal oxide clusters are in activating C–C and C–H bonds. For the Group VIII transition metals, the reactions of small $Fe_nCo_m^+$ clusters, $(n + m) \leq 3$, with C_2H_4O and O_2 in the gas phase have been investigated by Jacobson and Freiser using FT-ICR mass spectrometry.[3] Loh et al. studied the reactions of Fe_n^+ clusters ($n = 1-3$) with O_2 in a guided ion beam instrument. The reaction cross-sections measured as a function of kinetic energy were presented together with the thermochemistry.[4] The chemistry of size-selected Co_n^+ clusters ($n = 2-9$) with O_2 was studied by Guo et al. in a selected ion drift tube arrangement.[5] This work contains product distributions for the sequential oxidation reactions, as well as absolute reaction rates as a function of cluster size. Recently, Andersson et al. investigated the oxidation of neutral Fe_n, Co_n and Cu_n clusters ($n = 10-60$) in a molecular beam experiment.[6] Sticking probabilities S of O_2 were obtained as a function of cluster size. Fe_n and Co_n showed a comparable size dependence with S less than 0.2 for the smallest clusters. S increased almost monotonically up to $n = 25$, where it reached a constant value of 0.7 for Fe_n and 1.0 for Co_n.

Previous investigations in our laboratory had proved Fe_4^+ to be the outstanding cluster in the reactions of Fe_n^+ clusters ($n \leq 13$) with several reactants. Fe_4^+ was found to be the only cluster capable of dehydrogenation of NH_3[7] or C_6H_6[8] and of cyclotrimerisation of ethyne ligands to benzene.[9] Therefore, the following work is motivated by the question of whether Fe_4^+ will also show this special reactivity towards oxidising reagents. The earlier work on Fe_n^+ cluster oxidation was limited to sizes $n \leq 3$ and to O_2 as a reactant.[3,4] We studied the reactions of small Fe_n^+ clusters in the size range $n = 2-10$ with O_2, N_2O and CO_2. Thermochemical considerations allow the bracketing of dissociation energies for the Fe_n–O^+ bonds ($n = 2-6$). Although different reaction pathways are observed for the three X–O molecules, they all lead to final products of the same stoichiometry $Fe_xO_x^+$ ($x = 2-4$), which are unable to activate any further X–O bonds. Finally, mass-selected $Fe_xO_x^+$ ions ($x = 2$, 3) are exposed to C_6H_6, C_2H_4 and NH_3.

[*] Dr. M. P. Irion, Dipl.-Ing. O. Gehret
Institut für Physikalische Chemie, Technische Hochschule Darmstadt
Petersenstrasse 20, D-64287 Darmstadt (Germany)
Fax: Int. code + (6151) 16-6024

[**] This work is part of O. Gehret's dissertation (Darmstadt, D17).

0947-6539/96/0205-0598 $ 15.00+.25/0

Results and Discussion

Reaction Rates: The mass spectrum of Fe_n^+ clusters ($n = 3-19$) that have been sputtered, trapped and thermalised in our experimental setup is reproduced in ref. [10]. When the complete size distribution is exposed to one of the three X–O reactants, a multitude of products appears as a function of storage time. To obtain a clear relationship between reactants and products, we select the clusters before reaction according to their size.

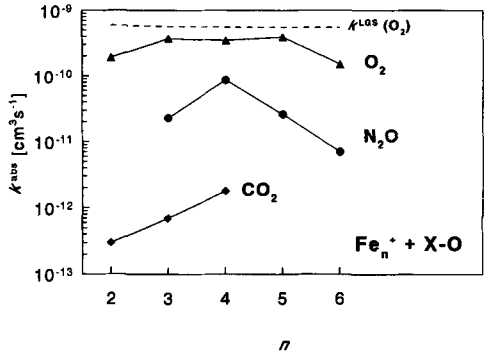

Fig. 1. Absolute rate constants for the reactions of Fe_n^+ clusters ($n = 2-6$) with O_2, N_2O and CO_2 as a function of size.

Figure 1 contains the absolute rates for the reaction of Fe_n^+ clusters ($n = 2-6$) with the X–O molecules as a function of size, derived from the disappearance of the naked cluster ions. As a reference, the collision rate calculated from Langevin theory[11] is plotted for the reaction of Fe_n^+ with O_2. From Figure 1, it is evident that the reaction rates strictly follow the order $k(O_2) > k(N_2O) > k(CO_2)$. With CO_2, reactions have been observed only for Fe_n^+ clusters in the size range $n = 2-4$. All sizes $n > 4$ appear inert under our experimental conditions ($k < 10^{-13}$ cm^{3}s^{-1}). However, clusters of all sizes react readily with O_2, and only Fe_2^+ appears inert towards N_2O. In all three reactions the rate increases from $n = 2$ to $n = 4$ for any given X–O molecule and passes a maximum at the size of the tetramer. This size dependence is least distinct for the fastest reaction (with O_2) and most distinct for the slowest reaction (with CO_2).

The reactions of Fe_n^+ clusters for $n > 6$ were investigated up to $n = 10$. When the whole size distribution was exposed to O_2 or N_2O, several oxide ions Fe_nO^+ ($n > 5$) did appear. However, it was not possible to monitor these reactions in detail because of the complexity and rapidity of consecutive reactions. For example, Fe_{10}^+ stored in the presence of N_2O yields $Fe_nO_m^+$ ions with $n = 3-10$ and $m = 1-4$. We have not measured reaction rates for $n > 6$, but we estimate them to approach the collision rate gradually with increasing size, as has been observed in other reaction systems.[1,19]

Reaction pathways: Figure 2 shows the pathways for the reactions of Fe_n^+ clusters ($n = 2-6$) with O_2. Clusters larger than Fe_6^+ are not included for the reasons pointed out above. The monomer Fe^+ has already been found to be inert by Kappes and Staley.[12]

For all clusters with $n > 3$, the addition of O_2 is accompanied in the first step by the loss of one or two Fe atoms. In the case of Fe_5^+ and Fe_6^+, the respective branching ratios amount to approximately 50%, as derived from the intermediates $Fe_{(n-1)}O_2^+$ and $Fe_{(n-2)}O_2^+$. The subsequent reaction steps of $Fe_5O_2^+$ and $Fe_4O_2^+$ lead to $Fe_4O_4^+$ and $Fe_3O_3^+$, respectively. The

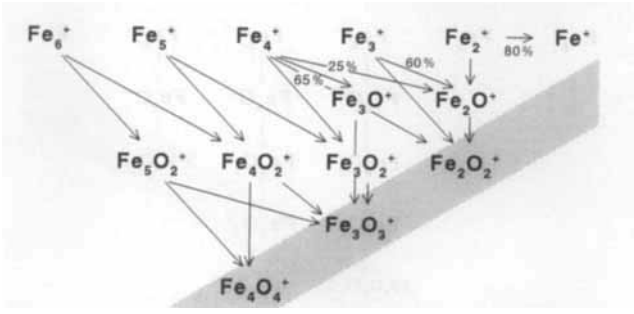

Fig. 2. Pathways observed for the reaction $Fe_n^+ + O_2$ ($n = 2-6$). If branching ratios are not indicated in percentages, a 1:1 ratio was found.

latter ions are found to be inert towards O_2. In the reaction with O_2, Fe_4^+ forms the products Fe_2O^+ (25%), $Fe_2O_2^+$ (65%), Fe_3O^+ (5%) and Fe_3O_2 (5%). In a second step, Fe_2O^+ forms $Fe_2O_2^+$, which does not react any further with O_2. Both Fe_3O^+ and $Fe_3O_2^+$ continue to react, yielding $Fe_3O_3^+$, which had already proved inert. Product ions Fe_2O^+ (60%) and $Fe_2O_2^+$ (40%) are also obtained through reaction of Fe_3^+ with O_2. In the presence of O_2, Fe_2^+ yields mainly Fe^+ (80%) and some Fe_2O^+ (20%), which completes the reaction by forming inert $Fe_2O_2^+$.

Thus, when Fe_n^+ clusters ($n = 2-6$) are stored in the presence of O_2, they react to give the stable final products $Fe_2O_2^+$, $Fe_3O_3^+$ and $Fe_4O_4^+$. Those ions that may form through different pathways are all inert towards further reaction with O_2. Beyond that, they are even inert towards every other X–O molecule examined. In the following, we will designate these $Fe_xO_x^+$ ions as "*microoxides of iron*".

Figure 3 contains the pathways for the reactions of Fe_n^+ ($n = 1-6$) with N_2O. Fe_2^+ appears inert, while for larger clusters almost every observed reaction step can be described as an O-atom transfer from N_2O inducing the loss of a single Fe atom

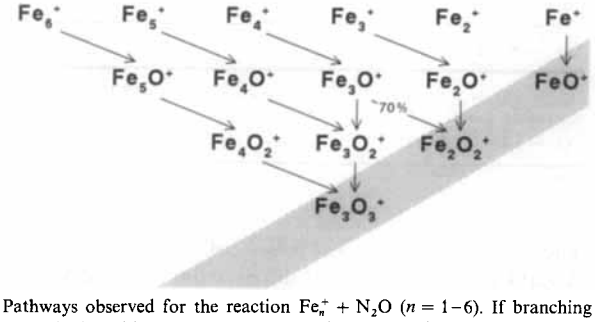

Fig. 3. Pathways observed for the reaction $Fe_n^+ + N_2O$ ($n = 1-6$). If branching ratios are not indicated in percentages, a 1:1 ratio was found.

and of N_2. Fe_6^+ clusters, for example, form $Fe_3O_3^+$ in three such consecutive steps. Exceptions to that rule are the ions Fe_3O^+, $Fe_3O_2^+$ and Fe_2O^+, which react with N_2O like the monomer Fe^+[12] (by inducing an O-atom transfer without loss of an Fe atom). Fe_3O^+ reacts to form $Fe_2O_2^+$ (70%) and $Fe_3O_2^+$ (30%). $Fe_3O_2^+$ and Fe_2O^+ continue to react until $Fe_3O_3^+$ and $Fe_2O_2^+$ are formed, respectively. These exclusive O-atom transfers seem to occur when $Fe_xO_x^+$ stoichiometry ($x = 1-3$) may be achieved. Thus, a product ion containing fewer iron than oxygen atoms is never observed.

The pathways for the reactions of Fe_n^+ with CO_2 are displayed in Figure 4. We observed consecutive reactions that consist of transfers of a single O atom to the Fe_n^+ cluster accompanied by the loss of CO. This stepwise buildup of oxides is terminated by $Fe_2O_2^+$ and $Fe_3O_3^+$ for Fe_2^+ and Fe_3^+, respectively. In the case of

  0947-6539/96/0205-0599 $ 15.00+.25/0

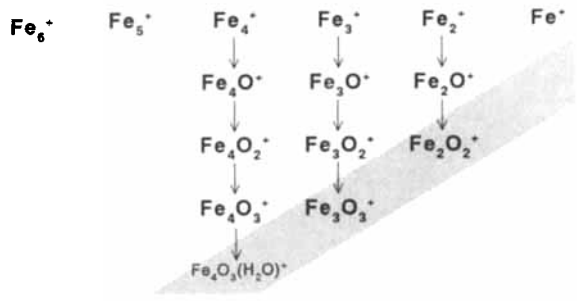

Fig. 4. Pathways observed for the reaction $Fe_n^+ + CO_2$ ($n = 2-4$).

Fe_4^+, the fourth ligand added under our experimental conditions was H_2O, resulting from a trace of water in the background vacuum.

From the results presented, we conclude that the patterns for the reactions of the Fe_n^+ clusters ($n = 2-6$) with any X–O molecule are characterised by a special type of reaction that depends strongly on the nature of the X–O reaction partner. Those characteristic types of reaction are as follows: in the case of O_2, two O atoms are transferred to the Fe_n^+ clusters, which lose up to two Fe atoms in the process. With N_2O, a single O-atom transfer occurs accompanied by the loss of one Fe atom and the liberation of an N_2 molecule. For CO_2, an O atom is simply transferred and CO is set free. These findings can now be discussed in terms of thermochemistry.

Thermochemical considerations: Since the reactivity of Fe_n^+ clusters towards X–O appears to follow the order $O_2 > N_2O > CO_2$, we attempt an explanation based on the dissociation enthalpies of the studied X–O bonds, which are contained in Table 1.[13]

Table 1. X–O bond dissociation enthalpies ΔH_D (kJ mol^{-1}) for X–O molecules [13].

XO → X + O	ΔH_D
$O_2 \rightarrow 2O$	+ 497.3
$N_2O \rightarrow N_2 + O$	+ 166.7
$CO_2 \rightarrow CO + O$	+ 531.7

The table suggests an order of enthalpies $\Delta H_D(CO_2) > \Delta H_D(O_2) > \Delta H_D(N_2O)$ that differs from the observed reactivity series. In order to gain a more thorough understanding, we will discuss qualitative potential energy surfaces for the reactions $Fe_4^+ + X-O$ that are compiled in Figure 5. In this discussion, we consider for O_2 the reaction path that leads to the main product $Fe_2O_2^+$, while for N_2O or CO_2 we consider the first reaction in the series, which leads to Fe_3O^+ and Fe_4O^+, respectively.

Generally, a chemical reaction starts with the collision of both reaction partners to form a collision complex. Under our experimental conditions, the collision frequency of the ions with the background gas was of the order of 1 s^{-1}. Therefore, the adsorption energy liberated in the obtained collision complex will not be quickly dissipated through collisions but will be distributed statistically over the degrees of freedom. Now, the excited collision complex may dissociate back into its components or proceed further on the reaction coordinate to be stabilised as a final product. The ratio of the experimental product formation rate to the theoretical collision rate[11] is usually termed reaction efficiency.

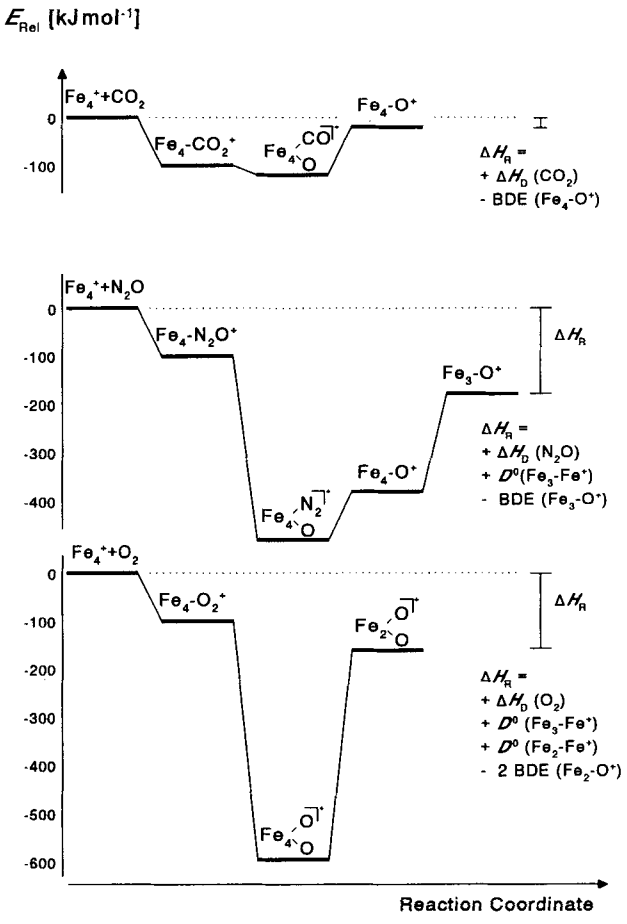

Fig. 5. Qualitative potential energy surfaces for
top: $Fe_4^+ + CO_2 \rightarrow Fe_4O^+ + CO$
centre: $Fe_4^+ + N_2O \rightarrow Fe_3O^+ + Fe + N_2$
bottom: $Fe_4^+ + O_2 \rightarrow Fe_2O_2^+ + Fe_2$
where ΔH_R is the reaction enthalpy of the net reaction and ΔH_D is the dissociation enthalpy of the X–O bond.

We are only able to detect the intensities of the longer-lived ions, namely of reactant and product ions. The lifetime of all intermediate ions along the reaction coordinate is about 0.1–1 μs and is by far too short for ICR detection. A recent example of a detailed investigation of a potential energy surface in transition-metal ion chemistry is given in ref. [14].

Thermalised ions undergo only exothermic reactions under gas-phase conditions like those we applied. In the following, we use the exothermicity of those reactions that occurred to derive lower limits for Fe_n-O^+ bond energies from our ICR measurements. A nonoccurring reaction may either be endothermic or be characterised by reaction barriers. Only if we assume the absence of such barriers may we use the nonoccurrence of certain reactions to derive upper limits for the desired bond energies.

In the reaction between Fe_4^+ and CO_2, a $[Fe_4-CO_2]^+$ collision complex is at first formed. CO_2 is activated by its binding with Fe_4^+, and one CO double bond is loosened. The obtained complex $[Fe_4(CO)(O)]^+$ then releases CO, decomposing to the final product Fe_4O^+. Therefore, it can be deduced from Figure 5 that the unknown Fe_4-O^+ BDE must be larger than or equal to 531.7 kJ mol^{-1}, the C–O dissociation enthalpy of CO_2.[13] To determine the upper limit of the BDE, we have to include the bond dissociation energies of the Fe_n^+ clusters. Table 2 contains the energies $D^0(Fe_{n-1}^+-Fe)$ for the loss of one Fe atom, measured by Lian et al. through CID for $n = 2-9$,[15]

0947-6539/96/0205-0600 $ 15.00+.25/0 Chem. Eur. J. 1996, 2, No. 5

Table 2. Bond dissociation energies D^0 (kJ mol^{-1}) for Fe_n^+ clusters ($n = 2-9$) [15].

Cluster	$D^0(Fe_{n-1}^+-Fe)$	$D^0(Fe_{n-1}^+-Fe)+D^0(Fe_{n-2}^+-Fe)$
Fe_2^+	264.4 ± 9.6	–
Fe_3^+	161.1 ± 11.6	425.5 ± 21.2
Fe_4^+	203.6 ± 19.3	364.7 ± 30.9
Fe_5^+	244.1 ± 22.2	447.7 ± 41.5
Fe_6^+	295.2 ± 24.1	539.3 ± 46.3
Fe_7^+	300.1 ± 26.1	595.3 ± 50.2
Fe_8^+	231.6 ± 26.1	531.7 ± 52.2
Fe_9^+	260.5 ± 31.8	492.1 ± 57.9

and the energies $D^0(Fe_{n-1}^+-Fe)+D^0(Fe_{n-2}^+-Fe)$ for the loss of two Fe atoms calculated therefrom. In this case, we use the process $Fe_4^+ \rightarrow Fe_4-O^+$ and the nonappearance of $Fe_5^+ \rightarrow Fe_4-O^+ + Fe$ to bracket the BDE (Fe_4-O^+) as $\Delta H_D(CO_2) + D^0(Fe_4-Fe^+) > BDE\ (Fe_4-O^+) > \Delta H_D(CO_2)$. Thus, we obtain $776 > BDE\ (Fe_4-O^+) > 531$ kJ mol^{-1}.

Fe_4^+ reacts with N_2O by forming the collision complex $[Fe_4-N_2O]^+$ in the first step (Fig. 5). Here, the Fe_4^+ cluster activates the N_2-O bond, producing the intermediate $[Fe_4(N_2)(O)]^+$. The net energy liberated in this process is provided by the emerging Fe_4-O^+ bond, diminished by the dissociation energy of N_2O (approximately 170 kJ mol^{-1}[13]). In the next step, N_2 loss occurs leading to $[Fe_4-O]^+$. The internal energy of the resulting $[Fe_4O]^+$ ion is large enough to expel a single Fe atom. Obviously, however, it is not large enough to initiate the loss of a second Fe atom. The final product detected is Fe_3O^+. We use the process $Fe_4^+ \rightarrow Fe_3O^+ + Fe$ in the reaction with N_2O and the nonappearance of Fe_3O^+ in the reaction of Fe_5^+ to bracket the $BDE(Fe_3-O^+)$ as $\Delta H_D(N_2O) + D^0(Fe_4-Fe^+) + D^0(Fe_3-Fe^+) > BDE(Fe_3-O^+) > \Delta H_D(N_2O) + D^0(Fe_3-Fe^+)$. Thus, we obtain $615 > BDE(Fe_3-O^+) > 370$ kJ mol^{-1}.

The reaction of Fe_4^+ with O_2 starts with the formation of the adduct $[Fe_4-O_2]^+$ (Fig. 5). The Fe_4^+ cluster activates the molecule that is bound dissociatively. The internal energy of the resulting $[Fe_4(O)_2]^+$ complex is high enough to release up to two Fe atoms. From the process $Fe_4^+ + O_2 \rightarrow Fe_2O_2^+ + 2Fe$, we obtain a lower limit for the average dissociation energy of the two Fe_2-O^+ bonds through $2 \times BDE(Fe_2-O^+) > D^0(Fe_3-Fe^+) + D^0(Fe_2-Fe^+) + \Delta H_D(O_2)$, so that $BDE(Fe_2-O^+) > 431$ kJ mol^{-1}. Furthermore, an upper limit may be derived from the nonoccurrence of the loss of three Fe atoms through $2 \times BDE(Fe_2-O^+) > D^0(Fe_4-Fe^+) + D^0(Fe_3-Fe^+) + D^0(Fe_2-Fe^+) + \Delta H_D(O_2)$. Obviously, this approach yields only average $BDE(Fe_n-O^+)$ values. The true bond dissociation energies will deviate from this value because they are certainly not identical for both oxygen atoms.

In a procedure similar to that applied for the Fe_4^+ clusters, BDE limits can also be derived for all other cluster sizes. Two reactions must be taken into account beside those discussed above. Firstly, the absence of the reaction $Fe_2^+ + N_2O \rightarrow Fe_2O^+ + N_2$ would require $BDE(Fe_2-O^+) < \Delta H_D(N_2O) = 166.6$ kJ mol^{-1}. Such a value would not allow the process $Fe_3^+ + N_2O \rightarrow Fe_2O^+ + Fe + N_2$ to occur. In this case, we can directly infer the existence of a reaction barrier. Armentrout et al. observed a kinetic barrier for oxygen abstraction from N_2O by monomer transition-metal ions and attributed it to spin multiplicity differences.[16] Secondly, the oxygen atom abstraction of Fe_2^+ from O_2 yields $BDE(Fe_2-O^+) > \Delta H_D(O_2) = 497.3$ kJ mol^{-1}. The BDE limits for Fe_n-O^+ ions ($n = 2-6$) we have obtained are summarised in Table 3. The highest of our lower limits and the lowest of our upper limits are plotted at each cluster size in Figure 6, which also contains the BDEs for Fe_n-O^+ ions ($n = 1-3$) given by Loh et al.[4,17]

Table 3. ICR bracketing limits for Fe_n-O^+ bond dissociation energies ($n = 2-6$) in kJ mol^{-1}. Numbers in bold indicate the highest lower limit and the lowest upper limit at a given cluster size.

	O_2 low	O_2 high	N_2O low	N_2O high	CO_2 low	CO_2 high
Fe_2-O^+	497	554	327	**532**	**531**	693
Fe_3-O^+	472	621	370	**615**	**531**	736
Fe_4-O^+	518	**669**	410	706	**531**	776
Fe_5-O^+	**546**	663	461	762	–	**532**
Fe_6-O^+	**514**	645	466	699	–	**532**

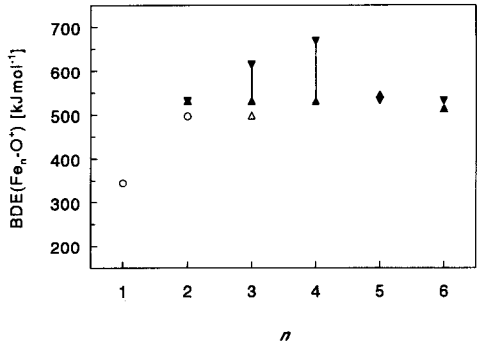

Fig. 6. Dissociation energies for the Fe_n-O^+ bond ($n = 1-6$) as a function of cluster size from ICR bracketing: lower (upper) limits represented by filled triangles with top up (down). Values measured by Loh et al. shown in comparison [4,17]: circles; lower limit for $n = 3$ is represented by an open triangle.

From the absolute reaction rates of all Fe_n^+ clusters ($n = 2-6$), the tetramer Fe_4^+ appears to be the most reactive cluster. This size effect is almost negligible for the reaction with O_2, where Fe_3^+ and Fe_5^+ react as fast as Fe_4^+. In the reactions with N_2O or CO_2, which are altogether slower, Fe_4^+ shows the highest rate over the whole size range. For Fe_5^+ and larger clusters, the rate of the reaction with CO_2 decreases below the detectable signal-to-noise level of our instrument. The uniqueness of the iron tetramer with respect to the rates is not so evident in the reaction pathways. Only with CO_2 is the tetramer unequivocally the largest reactive cluster. With N_2O and O_2, the pathways for Fe_4^+ do not differ from those shown by the other cluster sizes. The Fe_n-O^+ BDEs derived from the observed reaction pathways seem to drop slightly for $n > 4$, following the suppressed reactivity of Fe_5^+ and Fe_6^+ towards CO_2. However, the upper limits determined for the BDEs of Fe_5-O^+ and Fe_6-O^+ are uncertain, since the thermochemical thresholds may be shifted by barriers, as seen for the reaction of Fe_2^+ with N_2O. Taking this into account, we conclude that for $n \geq 2$ the average Fe_n-O^+ BDEs approach a nearly constant value without exhibiting a special size dependence.

The fact that $Fe_4O_4^+$ appears to be the largest $Fe_xO_x^+$ cluster does not suggest a kind of magic cluster size. The nonappearance of an $Fe_5O_5^+$ ion may be a result of the necessity for five consecutive reaction steps from Fe_{10}^+ in the reaction with N_2O. If an $Fe_5O_5^+$ ion resulted, it might have dissappeared below our signal-to-noise level. Even the $Fe_4O_4^+$ intensities we obtained in our mass spectra were so small as to render any further investigation of that species impossible.

Any further reactions of the oxidised clusters with X–O molecules do not differ significantly from those of the naked clusters. Generally, the consecutive reactions are driven by the tendency to reach $Fe_xO_x^+$ stoichiometry. For example, in the reaction of $Fe_5O_2^+$ with O_2 (Fig. 2), formation of the products $Fe_4O_4^+$ and $Fe_3O_3^+$ shows that the liberated bond energy is sufficient to release an Fe atom, or an Fe atom together with an FeO molecule. The spontaneity of the processes $Fe_3O_2^+ + O_2 \rightarrow Fe_3O_3^+ + O$ and $Fe_2O^+ + O_2 \rightarrow Fe_2O_2^+ + O$ suggests the for-

mation of $Fe_xO_x-O^+$ bonds ($x = 2, 3$) to be endothermic or impeded by significant reaction barriers. The intermediate ions $Fe_nO_m^+$ ($n = 2-4$; $m = 0-3$) in the reaction sequence with CO_2 (Fig. 4) must have BDEs > 531 kJ mol^{-1} for every additional oxygen atom up to $Fe_xO_x^+$ ($x = 2-4$).

Jacobson and Freiser also obtained $Fe_2O_2^+$, however, from the reaction of Fe_2^+ with ethylene oxide.[3] They generated Fe_2^+ clusters by reacting laser-desorbed Fe^+ ions with $Fe(CO)_5$. In the reaction of Fe_2^+ with O_2, they also observed the products $Fe^+ + FeO_2$ to be favoured over $Fe_2O^+ + O$. Interestingly, in contrast to our studies, Fe_2^+ appeared inert towards CO_2, consistent with the bond dissociation energy $D^0(Fe_2-O^+) = 496.9 \pm 4.8$ kJ mol^{-1} that was measured two years later by Armentrout and coworkers.[4] This may again provoke a discussion about the temperature of our metal clusters generated by sputtering.

We have already shown that in our experimental arrangement, sputtered metal cluster ions are thermalised to approximately room temperature.[18] A comparison of our recent results with those of Loh et al. supports this assertion.[4] They investigated the cross-sections for the oxidation of Fe_n^+ clusters ($n = 1-3$) by O_2 between 0 and about 15 eV of kinetic energy. From a comparison of their product ion ratios with ours, we deduce that the internal energy of our cluster ions is clearly below 0.4 eV relative to their energetic scale. Furthermore, our efficiencies for the reactions of Fe_2^+ and Fe_3^+ with O_2 equal within error limits those given in ref. [4]. Thus, we conclude that the sputtered clusters are almost completely thermalised under our experimental conditions. Nevertheless, the observed reactivity of Fe_2^+ towards CO_2 contradicts the assumption of a completely thermalised cluster ion population. Apparently, a small fraction of ions remains in excited states although collisional cooling does occur with pulsed-in Ne, background Xe and CO_2 itself. We observe a reaction efficiency of roughly 0.05%, which tells us that excited states may constitute at least 0.05% of the Fe_2^+ ions, since the reaction rate of the excited ions can be less than the theoretical rate.[11] However, this fraction should not exceed about 1% of the total ion population, since otherwise deviations from pseudo-first-order kinetics would be clearly visible. We have never observed such deviations for the reactions of Fe_n^+ clusters with O_2 or N_2O. Finally, the question remains whether the reactions of Fe_3^+ and Fe_4^+ are also influenced by excited-state chemistry. For metal clusters, the growing density of states with increasing cluster size should facilitate collisional cooling.[17] Thus, at least for Fe_4^+ clusters, hot ion chemistry does not play a role in the reactions with CO_2. Moreover it appears negligible for all other observed reactions of Fe_n^+ clusters with O_2 or N_2O.

Secondary reactions of $Fe_xO_x^+$ ions ($x = 2, 3$): In the following, we will discuss the reactions of the two oxidised iron cluster species with C_6H_6, C_2H_4 and NH_3. We will also compare the findings for these "microoxides" with the results obtained previously for the naked Fe_n^+ clusters.

The $Fe_xO_x^+$ ions ($x = 2, 3$) were generated through the reaction of size-selected Fe_4^+ clusters with N_2O, since this was the most efficient method of their production. As displayed in Figure 4, this reaction yields about 70% of $Fe_2O_2^+$ and 30% of $Fe_3O_3^+$. Unfortunately, we cannot isolate the $Fe_4O_4^+$ ion and study its further reactions, since its intensity is insufficient, even though it appears as a final product in the oxidation of Fe_5^+ or Fe_6^+ with O_2.

$Fe_xO_x^+ + C_6H_6$: Benzene is merely physisorbed by $Fe_xO_x^+$ clusters ($x = 2, 3$). C–H bond activation that would lead to dehydrogenation does not occur. During our experiments, we never observed the attachment of more than one benzene ligand to the oxide ions. Analogously, naked Fe_n^+ clusters do generally physisorb intact C_6H_6 as well. Only Fe_4^+ is able to activate the C–H bonds of benzene and dehydrogenate C_6H_6.[8] Thus in a first step, $Fe_4C_6H_4^+$ (65%) is formed beside $Fe_4C_6H_6^+$ (35%). After that, the Fe_4^+ clusters continue to react until they have attached up to four C_6 ligands. The upper part of Figure 7 summarises the pathways and rates for the reactions of the oxidised as well as of the naked iron clusters with benzene.

$Fe_xO_x^+ + C_2H_4$: Only $Fe_2O_2^+$ is found to react with ethene. In a dehydrogenation that occurs up to two times $Fe_2O_2(C_2H_2)_2^+$ is formed. The occurrence of this reaction is surprising, since of all naked Fe_n^+ clusters with $n \leq 13$ we have found only Fe_4^+ and Fe_5^+ to react with C_2H_4 in a similar way.[19] The reaction rates for Fe_4^+ and $Fe_2O_2^+$ are both comparable and about one order of magnitude larger than the rate for Fe_5^+. Whereas Fe_4^+ binds up to four, Fe_5^+ binds only up to two C_2H_2 ligands. The rates for the reactions with ethene are summarised in the lower part of Figure 7. The ion $Fe_3O_3^+$ proved unreactive towards ethene.

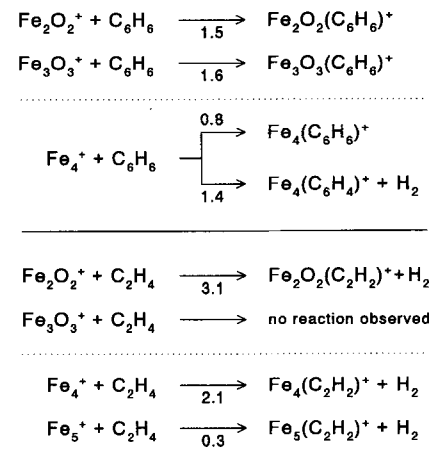

Fig. 7. Reactions observed for $Fe_xO_x^+$ ($x = 2, 3$) and Fe_4^+ clusters with C_6H_6 and with C_2H_4. Numerical values represent absolute reaction rates in 10^{-10} cm^3 s^{-1}.

$Fe_xO_x^+ + NH_3$: When Fe_4^+ is stored in the presence of approximately equal parts of N_2O and NH_3, the products shown in the reaction scheme in Figure 8 are obtained. Obviously, these are the same products that also appear in the reactions with only NH_3 or N_2O, namely $Fe_4(NH)^+$, $Fe_4(NH)_2^+$,[7] or $Fe_2O_2^+$, $Fe_3O_m^+$ ($m = 1-3$). In addition, mixed stoichiometries such as $Fe_2O(NH)^+$, $Fe_3O(NH)^+$, $Fe_3O(NH)^+$, $Fe_3O_2(NH)^+$, and $Fe_3O(NH)_2^+$, are observed. In analogy to the $Fe_xO_x^+$ clusters, mixed $Fe_xO_m(NH)_{x-m}^+$ product ions appear unable to activate any further N_2O or NH_3. Those ions persist with a mere physisorption of intact ammonia.

Of all observed products in the upper part of Figure 8, the appearance of the $Fe_2O(NH)^+$ ion is most remarkable. This ion could result from a reaction of Fe_3O^+ with NH_3, accompanied by the loss of an Fe atom. Since Fe_4^+ attaches NH from NH_3 without Fe atom loss,[7] $Fe_2O_2^+$ was mass-selected and NH_3 introduced through a pulsed valve to clarify the origin of the $Fe_2O(NH)^+$ ion. The startling result is that it emerges from a ligand exchange process (lower part of Fig. 8)! NH_3 displaces an O ligand, attaching the isosteric NH and expelling H_2, which binds the former O ligand to produce an H_2O molecule. Since only exothermic reactions occur spontaneously in the gas phase, the observed H_2O formation must be

0947-6539/96/0205-0602 $ 15.00+.25/0 Chem. Eur. J. 1996, 2, No. 5

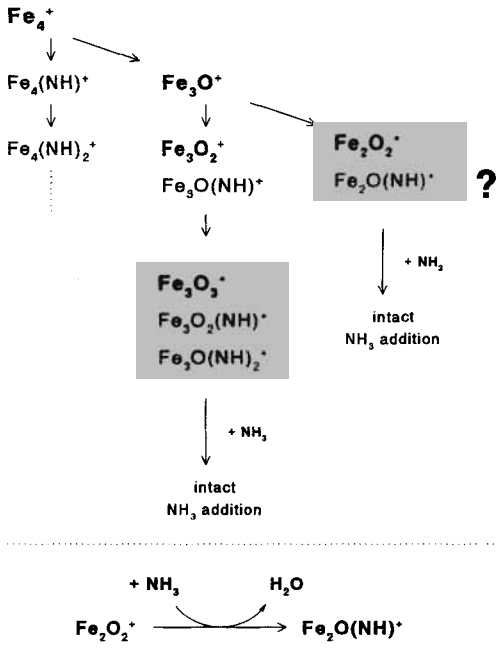

Fig. 8. Top: Products observed when Fe_4^+ is stored in the presence of NH_3 and N_2O. Bottom: Ligand exchange of mass-selected $Fe_2O_2^+$ with NH_3.

exothermic. Otherwise, if H_2 were abstracted together with an O atom, the ligand exchange would have to be endothermic. This process is also surprising because naked Fe_2^+ clusters are unable to activate NH_3. The exchange of an oxo with an imido ligand has been observed previously at the Fe^+ ion by Freiser and coworkers.[20] Furthermore, it is evident in our studies that the $Fe_3O_3^+$ ion does not undergo such a ligand exchange reaction.

Further understanding may be gained from knowledge of the geometric or electronic structure of the $Fe_xO_x^+$ ions. Recently, Castro et al. reported density-functional calculations for Fe_n, Fe_n^+ and Fe_n^- clusters of sizes $n \leq 5$.[21] They obtained lowest-energy structures for maximum numbers of nearest-neighbour bonds. To our knowledge, similar data on the bonding of oxygen to transition-metal clusters are not available. Therefore, it is appropriate to look at common coordination chemistry that suggests an O-atom-bridging type of bonding.[22] This is also backed up by the Fe_n–O^+ BDEs we determined as roughly 550 kJ mol^{-1} (Fig. 6) that are significantly higher than the monomer Fe–O^+ value of around 350 kJ mol^{-1}.[4] From this resoning, we deduce structures **1** and **2** (Scheme 1), which had already been predicted by Jacobson and Freiser.[3] The cubane-like structure **3** is well-known for M_4S_4 species (M = Mo, Fe, Co) and may therefore be predicted for $Fe_4O_4^+$ as well, although a μ_3-bridging O atom has been reported in coordination chemistry only for a rhenium complex.[22,23] Based on the assumed planar structures **1** and **2**, a single C_6H_6 ligand may be added by a loose coordination with its π-electron cloud parallel to the oxide plane. The fact that $Fe_2O_2^+$ binds up to two C_2H_2 ligands may be explained by the coordination of a single ligand to each Fe atom. The experimental finding that only one NH ligand exchanges with a bridging O atom and leads to molecule **4** is not yet understood. The inert behaviour of $Fe_3O_3^+$ (**2**) may be due to

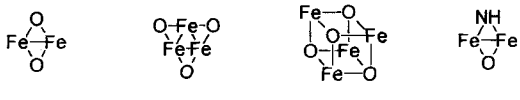

1 **2** **3** **4**

Scheme 1. Structures assumed for oxidised iron cluster cations.

both electronic and geometric factors. On one hand, each Fe atom in **2** possesses two metal–metal bonds and on the other hand, the O-atom bridges in **2** screen a larger part of the metal centre than those in **1** do. As mass spectrometry does not provide direct structural information and calculations on metal cluster ion reactions are not available yet, we are left to mere speculation.

Experimental Procedure

Details of the experimental setup have already been described [24]. Briefly, bare metal cluster cations were produced by sputtering a metal target with Xe^+ primary ions at about 20 keV kinetic energy. They were injected into the storage cell of our FT-ICR instrument through an electrostatic lens arrangement. Altering the potential of a front grid allows the controlled admission of metal cluster ions to the cell. In the experiments described here, the ICR cell was usually filled for about 2 s and Ne gas was pulsed in through a piezoelectric valve to decelerate and cool the clusters. The complete ensemble of stored Fe_n^+ cluster ions contained the sizes $n = 3$–19 [10]. In the subsequent period, the clusters underwent collisions with the rare gas atoms forming a heat sink at roughly room temperature and finally achieved thermal equilibrium [18]. Before investigation of their chemistry, clusters were size-selected by removal of all undesired sizes by means of wide-band radio-frequency ejection pulses. Reactant gases were generally admitted by raising the background pressure of less than 10^{-9} mbar up to a given steady-state value through a continuous leak valve. A pulsed valve was used for this purpose only in special cases. After a reaction delay an excitation pulse followed and initiated detection of all ions present in the cell.

For the determination of reaction rate constants, size-selected clusters were stored in the presence of O_2 (6×10^{-9} mbar), N_2O (2×10^{-8} mbar) or CO_2 (1×10^{-7} mbar) for up to 90 s. Relative rate constants were calculated from the decrease of Fe_n^+ cluster intensities, assuming pseudo-first-order kinetics. From these, we obtained absolute reaction rates by measuring the partial pressure of the reactants with a calibrated ionisation gauge [25]. Mainly because of the uncertainty of this pressure determination, the error in the absolute reaction rates is estimated to be about $\pm 50\%$. Reaction pathways were obtained by monitoring product ion intensities as a function of storage time.

Acknowledgements: This work was generously supported by the Deutsche Forschungsgemeinschaft and the Fonds der Chemischen Industrie.

Received: May 26, 1995
Revised version: September 12, 1995 [F138]

[1] See for example: D. C. Parent, S. L. Anderson, *Chem. Rev.* **1992**, *92*, 1541; A. Kaldor, D. M. Cox, M. R. Zakin, *Adv. Chem. Phys.* **1988**, *70*, 211.
[2] D. Schröder, H. Schwarz, *Angew. Chem. Int. Ed. Engl.*, **1995**, *34*, 1973.
[3] D. B. Jacobson, B. S. Freiser, *J. Am. Chem. Soc.* **1986**, *108*, 27.
[4] S. K. Loh, L. Lian, P. B. Armentrout, *J. Chem. Phys.* **1989**, *91*, 6148.
[5] B. C. Guo, K. P. Kerns, A. W. Castleman, Jr., *J. Phys. Chem.* **1992**, *96*, 6931.
[6] M. Andersson, J. L. Persson, *Nanostruct. Mater.* **1993**, *3*, 337.
[7] M. P. Irion, P. Schnabel, *J. Phys. Chem.* **1991**, *95*, 10596.
[8] O. Gehret, M. P. Irion, *Chem. Phys. Lett.*, in press.
[9] P. Schnabel, K. G. Weil, M. P. Irion, *Angew. Chem.* **1992**, *104*, 633; *Angew. Chem. Int. Ed. Engl.* **1992**, *31*, 636.
[10] A. Selinger, P. Schnabel, W. Wiese, M. P. Irion, *Ber. Bunsenges. Phys. Chem.* **1990**, *94*, 1278.
[11] P. Langevin, *Ann. Chim. Phys.* **1905**, *5*, 245; G. Gioumousis, D. P. Stevenson, *J. Chem. Phys.* **1958**, *29*, 294.
[12] M. M. Kappes, R. H. Staley, *J. Am. Chem. Soc.* **1981**, *103*, 1286.
[13] *CRC Handbook of Chemistry and Physics* (Ed.: D. R. Lide), Boston, **1991**.
[14] M. R. Sievers, P. B. Armentrout, *J. Chem. Phys.* **1995**, *102*, 754.
[15] L. Lian, C.-X. Su, P. B. Armentrout, *J. Chem. Phys.* **1992**, *97*, 4072.
[16] P. B. Armentrout, L. F. Halle, J. L. Beauchamp, *J. Chem. Phys.* **1982**, *76*, 2449; P. B. Armentrout, *Annu. Rev. Phys. Chem.* **1990**, *41*, 313.
[17] S. K. Loh, E. R. Fisher, L. Lian, R. H. Shultz, P. B. Armentrout, *J. Phys. Chem.* **1989**, *93*, 3159.
[18] P. Schnabel, M. P. Irion, K. G. Weil, *Ber. Bunsenges. Phys. Chem.* **1991**, *95*, 197.
[19] P. Schnabel, M. P. Irion, *Ber. Bunsenges. Phys. Chem.* **1992**, *96*, 1101.
[20] S. W. Buckner, J. R. Gord, B. S. Freiser, *J. Am. Chem. Phys.* **1988**, *110*, 6606.
[21] M. Castro, D. R. Salahub, *Phys. Rev. B* **1994**, *49*, 11842.
[22] C. Elschenbroich, A. Salzer, *Organometallchemie*, Teubner, Stuttgart, **1993**.
[23] E. L. Muetterties, T. N. Rhodin, E. Band, C. F. Bruckner, W. R. Pretzer, *Chem. Rev.* **1979**, *79*, 91.
[24] M. P. Irion, A. Selinger, R. Wendel, *Int. J. Mass Spectrom. Ion Processes* **1990**, *96*, 27.
[25] J. E. Bartmess, R. M. Georgiadis, *Vacuum* **1983**, *33*, 149.